Laser frequency analysis aided by electronic frequency dividers

Dipen Barot, *Member, IEEE* and Lingze Duan, *Senior Member, IEEE*

***Abstract*— Conventional laser spectral analysis relies on direct measurement of power spectral density (PSD), which is not able to distinguish certain types of phase and frequency modulations without ambiguity. In this paper, we propose and demonstrate a modified scheme aimed at improving the specificity in laser frequency analysis. Our method is based on PSD measurement of the downshifted laser spectrum in the radio-frequency range but introduces an electronic frequency divider (EFD) prior to the spectrum analyzer. By monitoring the spectral changes caused by the EFD, we show, both theoretically and experimentally, that common scenarios of phase and frequency modulations, such as wideband frequency modulation (FM) and broadband phase modulation, can be differentiated without ambiguity. Moreover, the new method allows for quantitative assessment of wideband FM parameters such as modulation frequency, modulation index and frequency deviation, which is not possible with any conventional spectral analysis methods. This technique may find potential applications in laser frequency metrology, microwave photonics, optical sensing, and radar/lidar technologies.**

***Index Terms*—Frequency division, frequency measurement, frequency modulation, laser noise, microwave photonics, phase noise, radar, spectral analysis.**

I. Introduction

ULTRALOW-noise and ultra-stable sources of reference signals in the optical domain have become indispensable for applications such as precision measurements, optical frequency metrology, coherent optical communications, and microwave photonics [1]. As the demand for such high-spectral-purity light sources continues to increase, there arises the need for instrumentation with improved capabilities in characterizing key performance metrics of these sources. One area of particular interest is the specificity in laser phase/frequency noise (PFN) measurement.

Various techniques have been exploited to determine the PFN of lasers. In the optical domain, the most straightforward approach is the delay-line scheme, in which an interferometer with highly imbalanced arm lengths is combined with a homodyne (or heterodyne) detector for linewidth evaluation [2]–[4]. Despite its simplicity and cost effectiveness, this method is only suitable for characterizing the Lorentzian linewidth of a source and is unable to provide a true picture of the PFN when the source is subject to large frequency modulations (FM) [5]. Other optical schemes to measure PFN usually rely on optical frequency discriminators (OFD), which convert PFN into amplitude variations. Typical OFDs are gratings [6], optical resonators [7], as well as atomic transitions [8]. Methods based on OFDs are low cost and easy to implement, but they suffer from limitations in frequency resolution, signal to noise ratio and stability [9]. Laser PFN can also be measured in the radio-frequency (RF) range by employing appropriate frequency downshifting [9], [10]. The downshifting is normally accomplished by heterodyning the laser under test with a reference laser to produce a beat note at the difference frequency. It can also be done with the help of certain optoelectronic devices such as a photoconductive mixer [11], [12]. The RF methods typically have much higher frequency resolutions and signal-to-noise ratios compared to the OFD-based methods [3]. Its drawbacks in system complexity and cost have also been significantly mitigated in recent years by the advance in optical frequency comb technologies [13].

From a fundamental point of view, all of these conventional methods ultimately rely on direct measurement of power spectral density (PSD) of modulation sidebands to characterize phase and frequency fluctuations. As a result, they suffer from a common limitation, which is the intrinsic ambiguity between FM modulation frequency and instantaneous frequency. This can be understood by the fact that knowing solely the PSD of a modulation sideband cannot lead to a definitive distinction between a broadband noise source with a low modulation index across its entire bandwidth (known as a broadband phase modulation) and a low-frequency fluctuation with a very large modulation index (known as a wideband FM). Moreover, in the latter case, conventional methods are incapable of providing quantitative assessment of key FM parameters such as modulation frequency and modulation index. Yet, in practice, information about the nature and the scale of noise sources is often critical for pinning down their causes and mitigating them. For example, when designing active locking systems for laser frequency stabilization, it is paramount to understand the exact factors contributing to laser instability and their scales [14]. Systems optimized to suppress slow but large frequency modulations are typically different from systems optimized to suppress broadband phase noise. Unfortunately, this kind of assessment is often performed in the labs based on experience and repeated tests.

This work was supported in part by the National Science Foundation under Grants ECCS-1254902 and 1606836.

The authors are with the Physics Department, the University of Alabama in Huntsville, Huntsville, AL 35899 USA (e-mail: lingze.duan@uah.edu).

In this report, we present a simple but elegant method to improve the specificity of laser spectral analysis. Our method is based on the RF-discriminator scheme mentioned above but makes a crucial change by introducing an electronic frequency divider (EFD) before the PSD measurement. EFD is a common electronic component that is widely available in a variety of forms and packages (e.g., Analog Devices HMC Series). Interested readers can find detailed descriptions about EFD in classic papers such as [15] and [16]. By showing the differences in the response of EFD to various FM scenarios, we demonstrate the feasibility to differentiate common laser PFN situations and quantify large FM parameters via a simple modification to the existing technique.

The paper is organized as follows. In Section II, we present a theoretical description of angle-modulated signals under the operation of frequency division and outline the principle of the proposed technique. Section III describes an experiment that verifies the theory developed in Section II. Section IV reports a case study in which our technique is applied to the frequency analysis of a realistic laser beat note. Finally, we conclude in Section V.

II. Principle of Operation

In this section, we first overview the mathematical framework for *angle modulation* (a general term for phase and frequency modulations [17]). We then discuss the limitations of conventional PSD measurement. After that, we describe the effects of frequency division in various modulation scenarios. Finally, we present the operating principle of the new method.

A. Mathematical Framework

In general, a sinusoidal carrier with constant amplitude but time-varying phase can be mathematically described by [17]

$$x(t) = A_c \exp\left[j\theta(t) \right] = A_c \exp\left\{ j\left[2\pi f_c t + \phi(t) \right] \right\}, \quad (1)$$

where A_c is carrier amplitude, $\theta(t)$ is total instantaneous angle, f_c is carrier frequency, and $\phi(t)$ is time-dependent phase angle. If the phase is subject to a modulation, it can be further expressed as

$$\phi(t) = 2\pi K_f \int_0^t m(\tau)\, d\tau, \quad (2)$$

where K_f is frequency sensitivity of the modulator and $m(\tau)$ is the modulation signal. The instantaneous frequency of the signal is defined as

$$f(t) \equiv \frac{1}{2\pi}\dot{\theta}(t) = f_c + K_f m(t). \quad (3)$$

Since an arbitrary modulation signal can be decomposed into a collection of single-frequency components via Fourier transform, it is worthwhile to take a closer look at the so called tone modulation, where $m(\tau)$ takes the form of a sinusoidal function $m(\tau) = A_m \cos(2\pi f_m \tau)$, with A_m being modulation amplitude and f_m representing modulation frequency. Then (1) can be rewritten as

$$x(t) = A_c \exp\left(j2\pi f_c t \right) \cdot \exp\left[j\beta \sin(2\pi f_m t) \right], \quad (4)$$

where $\beta = K_f A_m / f_m$ is commonly known as modulation index. By defining peak FM frequency deviation $\Delta f \equiv K_f A_m$, modulation index can also be expressed as $\beta = \Delta f / f_m$. Expanding the second exponential term in (4) into an infinite series yields [17]

$$x(t) = A_c \sum_{n=-\infty}^{+\infty} J_n(\beta) \exp\left[j2\pi \left(f_c + n f_m \right) t \right], \quad (5)$$

where $J_n(\beta)$ is Bessel's function of the first kind of order n and argument β. In the special case of small modulation index, i.e., $\beta << 1$, all terms except the 0th and the 1st orders in (5) are negligible, yielding

$$x(t) \approx A_c \left\{ J_0(\beta) \exp\left(j2\pi f_c t \right) \pm J_1(\beta) \exp\left[j2\pi \left(f_c \pm f_m \right) t \right] \right\} \quad (6)$$

Fourier transform of (6) gives the spectrum of the signal,

$$X(f) = \frac{A_c}{2}\left[J_0(\beta)\delta\left(f - f_c \right) \pm J_1(\beta)\delta\left(f - f_c \mp f_m \right) \right], \quad (7)$$

which consists of the carrier f_c along with two sidebands at $f_c \pm f_m$.

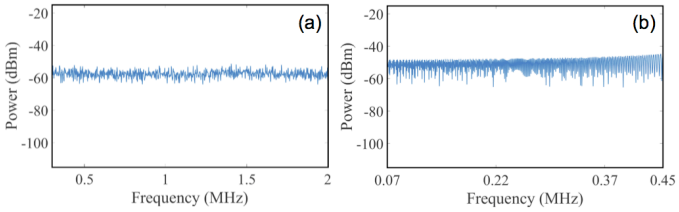

Fig. 1. Ambiguity in direct PSD measurement: (a) the PSD of a white phase noise, and (b) the PSD caused by a wideband tone-modulation. Both spectra are recorded with a Tektronix MDO 4104B mixed domain oscilloscope with a resolution bandwidth of 300 Hz.

B. Limitations of Direct PSD Measurement

In the current context, we are specifically interested in the comparison between two hypothetical scenarios. The first scenario is a broadband modulation with a constant but small modulation index (i.e., $\beta << 1$) across the entire modulation band. In reality, this closely resembles the case of white phase noise. According to (7), each Fourier component (denoted here as f_i) of such a modulation generates a pair of sidebands at $f_c \pm f_i$ with an amplitude equal to $(A_c/2)J_1(\beta)$, which is a constant. As a result, the overall sideband, after considering all possible values of f_i, has a constant PSD throughout its span. Such a feature is demonstrated in Fig. 1(a), which shows the measured PSD of a white phase-noise sideband.

The second scenario is a single-tone modulation at f_m, with a frequency deviation $\Delta f >> f_m$ and hence a modulation index $\beta >> 1$. The spectral feature due to this modulation is better captured by invoking the concept of instantaneous frequency. According to (3), the instantaneous frequency under such a modulation is given by $f(t) = f_c + \Delta f \cos(2\pi f_m t)$, which represents a frequency sweep between $f_c \pm \Delta f$ at a rate of f_m.

A direct measurement of the signal spectrum would result in a constant PSD throughout the frequency sweeping range, as demonstrated in Fig. 1(b).

The above two scenarios show that completely different fluctuation mechanisms may yield very similar PSD profiles under direct PSD measurement, which can potentially cause ambiguity in practice. Such a limitation of the conventional methods is particularly problematic for high precision laser frequency analysis, where the nature of the fluctuation in question is often critical for determining effective approaches of mitigation. Methods capable of improving the specificity of PSD measurement thus become highly desirable.

C. *The Effects of Frequency Division*

Now let us analyze how the operation of frequency division impacts an angle-modulated signal. Once again, we focus on the case of tone modulation with the understanding that a general modulation scenario can always be decomposed into a collection of tone modulations through the Fourier transform. Consider a single-tone-modulated signal as shown in (4). When it passes through a frequency divider with a division ratio N, both terms on the exponents are divided by N and the output signal is given by

$$y(t) = A_c \exp\left(j2\pi \frac{f_c}{N} t \right) \cdot \exp\left[j \frac{\beta}{N} \sin(2\pi f_m t) \right]. \quad (8)$$

A similar series expansion as the one performed on (4) yields

$$y(t) = A_c \sum_{n=-\infty}^{+\infty} J_n\left(\frac{\beta}{N} \right) \exp\left[j2\pi \left(\frac{f_c}{N} + n f_m \right) t \right]. \quad (9)$$

Taking the Fourier transform of (9) results in an expression for the spectrum of a tone-modulated sinusoidal carrier after an N-fold frequency division,

$$Y(f) = \frac{A_c}{2} \sum_{n=-\infty}^{+\infty} J_n\left(\frac{\beta}{N} \right) \delta\left[f - \left(\frac{f_c}{N} + n f_m \right) \right]. \quad (10)$$

Equations (10) shows that frequency division causes two changes on a tone-modulated signal: it divides the carrier frequency f_c by N and it divides the modulation index β by N. On the other hand, frequency division does *not* change the modulation frequency f_m and hence the sideband spacing remains the same.

The effect of frequency division can also be understood through the concept of instantaneous angle and instantaneous frequency defined in (1) and (3). A divider effectively divides $\theta(t)$ and $f(t)$ by its division ratio N. For tone modulation, the divided instantaneous frequency becomes

$$\frac{f(t)}{N} = \frac{f_c}{N} + \frac{\Delta f}{N} \cos(2\pi f_m t). \quad (11)$$

From the viewpoint of frequency sweeping, this indicates that the operation of frequency division causes a reduction of both the carrier frequency and the frequency sweeping range by the same ratio. However, it should be noted that such a picture is only valid when $\Delta f / N >> f_m$, which essentially requires both $\beta >> 1$ and $\beta / N >> 1$. A comparison between (10) and (11) also indicates that a division of β is equivalent to a division of Δf.

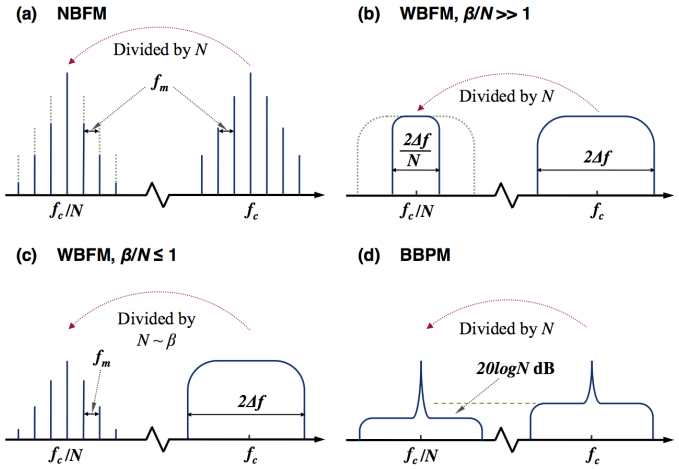

Fig. 2. The effects of frequency division in different angle-modulation scenarios: (a) a reduction of sideband amplitude (vertical) in the case of narrowband tone modulation; (b) a reduction of frequency span (horizontal) in the case of wideband tone modulation and small division ratios; (c) a change of characteristics from frequency sweeping to discrete sidebands in the case of wideband tone modulation and large division ratios; and (d) a universal reduction of sideband amplitude (by 20log$N$ dB in PSD scale) in the case of broadband phase modulation.

D. *Spectral Changes due to Frequency Division*

With the understanding of the effects of frequency division, let us now examine the spectral changes caused by frequency dividers under various circumstances. We shall broadly group these different scenarios into two categories: *tone modulation* and *broadband modulation*. Within tone modulation, we further break down the discussion into three different cases based on the relative scales of the modulation index and the division ratio:

1) *Narrowband FM (NBFM)*
This is the case where the FM frequency deviation is small compared to the modulation frequency, i.e., $\Delta f \le f_m$, or equivalently, $\beta \le 1$. According to (5), the modulation can be treated as consisting of a series of harmonic components at the multiples of f_m. Moreover, since β is small, only the first few orders of Bessel's function have significant contributions in the expansion. As a result, the original spectrum consists of several discrete sidebands on both sides of the carrier. The frequency-divided signal is described by (10), where the carrier frequency and the modulation index are both divided by N. The modulation frequency, however, remains unchanged. The result is a second set of discrete sidebands centered at f_c / N, with the same sideband spacing but reduced amplitudes. Such a spectral change is illustrated in Fig. 2(a). Evidently, the main characteristic difference before and after the divider is a reduction in the "vertical" scale of the sidebands (i.e., amplitude or power).

2) *Wideband FM (WBFM) with small division ratio*
This is the case where the FM frequency deviation is large compared to the modulation frequency, i.e. $\Delta f >> f_m$ and

$\beta >> 1$, but the division ratio N is small relative to β so that $\beta / N >> 1$. Under such conditions, it is more convenient to use the concept of instantaneous frequency defined in (3) and treat the modulation as a frequency sweeping, both before and after the divider. The effect of a frequency divider can be described by (11), which indicates a simultaneous reduction of the carrier frequency and the frequency-sweeping range, as illustrated in Fig. 2(b). Clearly, the main characteristic change in the spectrum is a reduction in the "horizontal" scale (i.e., frequency span).

3) *WBFM with large division ratio*
This case is similar to the previous one except the division ratio N becomes comparable to or greater than β so that $\beta / N \le 1$. The original signal has a large β and acts as a frequency sweeping. But the divided modulation index is so small that the divided spectrum only consists of discrete sidebands, as conceptually depicted in Fig. 2(c). Evidently, such a characteristic transition requires the division ratio to be at least comparable to the original modulation index, i.e., $N \approx \beta$. This interesting feature can be used to quantify the scale of β as will be discussed in the following.

As a summary of tone modulation, the above three cases can also be qualitatively understood through the so-called Carson's rule [17], which states that the bandwidth of an angle-modulated signal can be approximately predicted by the relation $BW \approx 2 f_m (\beta + 1)$. When $\beta << 1$, the bandwidth is dominated by the second term on the right-hand side so that $BW \approx 2 f_m$. Since f_m does not change through frequency division, the signal bandwidth remains the same after the divider while the sideband amplitudes reduce. On the other hand, when $\beta >> 1$, the first term in the parentheses dominates so that $BW \approx 2 f_m \beta = 2\Delta f$. Now the bandwidth is mainly determined by the FM frequency deviation Δf, which defines the span of frequency sweeping. Under frequency division, the bandwidth reduces following the reduction of β (and hence Δf). However, once β / N becomes comparable to 1, the first term is no longer dominant and discrete sidebands once again appear in the spectrum.

Finally, the above discussions based on single-tone modulation in principle also apply to multi-tone and broadband modulations. In particular, broadband modulations with small index are especially common in practice and hence should be discussed separately.

4) *Broadband phase modulation (BBPM)*
This is the case where the modulation is composed of a continuous band of f_m and $\beta << 1$ holds true across the entire band. This case can be more conveniently described by directly invoking (1) and assuming $\phi(t) = \phi_\Delta a(t)$, where ϕ_Δ represents the maximum phase shift produced by a general modulation function $a(t)$ with $\phi_\Delta \le \pi$. It is straightforward to show that [17], as long as $|\phi(t) << 1|$ is satisfied (which leads to the name *phase modulation*), the Fourier transform of $x(t)$ can in general be written as

$$X(f) = \frac{A_c}{2}\left[\delta\left(f - f_c\right) + j\phi_\Delta A\left(f - f_c\right)\right], \tag{12}$$

where $A(f)$ is the Fourier transform of $a(t)$. With an N-fold frequency division, f_c and ϕ_Δ are both divided by N, and signal spectrum becomes

$$X_{1/N}(f) = \frac{A_c}{2}\left[\delta\left(f - \frac{f_c}{N}\right) + j\frac{\phi_\Delta}{N} A\left(f - \frac{f_c}{N}\right)\right]. \tag{13}$$

Apparently, the entire sideband downshifts to a new center frequency f_c / N, with a universally reduced amplitude ϕ_Δ / N. The characteristic change of the spectrum is a reduction in the "vertical" scale, as depicted in Fig. 2(d), which is in essence similar to the behavior of NBFM except this is for a continuous band. It is also interesting to point out that, according to (13), the PSD of the divided spectrum has an identical profile as the undivided spectrum but $20\log_{10} N$ dB lower.

E. Operating Principle of EFD-Aided Frequency Analysis

Overall, the characteristic difference in spectral behaviors under frequency division makes it possible to distinguish different types of angle modulation by means of frequency dividers. Especially, in the context of laser frequency analysis, by introducing an EFD preceding a spectrum analyzer and comparing the PSD measurements with and without the EFD, one can easily draw distinctions between a laser spectrum caused by slow but large frequency fluctuations (Fig. 2(b)) and a laser spectrum dominated by white phase noise (Fig. 2(d)). Such differentiation cannot be accomplished without ambiguity with the conventional direct PSD measurement as pointed out in Section II *B*. Moreover, by finding that "magic" division ratio N at which a WBFM sideband transitions into a NBFM sideband as shown in Fig. 2(c), one can deduce the approximate value of β through the relation $\beta \approx N$. The resulted NBFM spectrum allows for easy determination of f_m (keeping in mind that f_m remains invariant through frequency division). The FM frequency deviation, Δf, can be estimated based on the relation $\beta = \Delta f / f_m$. Evidently, the approach outlined above enables systematical decoding of the modulation parameters of an arbitrary WBFM signal, which is not possible using any conventional spectral analysis methods.

III. Experiment Verification

In order to verify the capability of EFD-aided frequency analysis in discriminating various types of angle modulation and quantifying WBFM parameters, we set up an experiment in which an arbitrary angle-modulated signal can be loaded onto low-noise laser light. We then use the EFD-aided method to measure the laser spectrum and compare it with theoretical predictions.

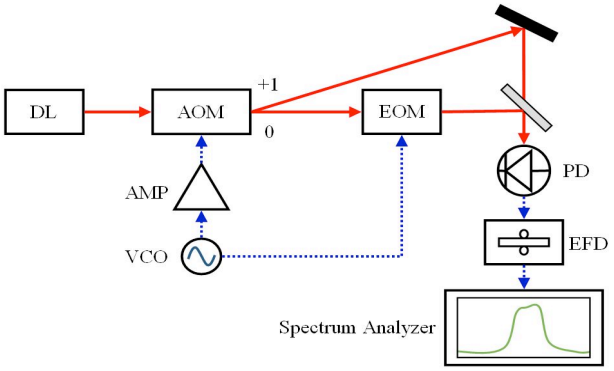

Fig. 3. Schematic of experimental setup. AMP: RF amplifier; AOM: acousto-optic modulator; DL: diode laser; EOM: electro-optic phase modulator; PD: photodetector; VCO: voltage-controlled oscillator. Solid red lines represent optical paths and dotted blue lines represent electronic paths.

Fig. 3 shows a schematic of the experimental system. The light source is a narrow-linewidth, low-noise diode laser (RIO Orion, < 1 kHz linewidth). An acousto-optic modulator (AOM) splits the laser output into two beams with a frequency offset governed by the driving signal of the AOM. The AOM is driven by a voltage-controlled oscillator (VCO) operating at 80 MHz. FM can be applied to the +1-order output of the AOM by modulating the control voltage of the VCO. The 0th-order output of the AOM passes through an electro-optic phase modulator (EOM), which provides an alternative port for loading BBPM onto the laser light. The two beams recombine on a photodetector, which serves as a heterodyne receiver to downshift the laser spectrum to the RF band so that it can be analyzed by EFDs. Two programmable EFDs (Valon 3008) are used, each with a maximum division ratio of 32. When arranged in series, they are able to provide an overall frequency division up to 1024. The divided laser spectra are saved and analyzed with an RF spectrum analyzer (Tektronix RSA 306B).

Fig. 4 summarizes the main results of the experiment. In order to make comparisons with theory, we plot all traces as single-sided spectra, with solid black traces representing experimental results and dashed red traces representing theoretical predictions. Fig. 4(a) and (b) correspond to the case of NBFM, where the phase of the laser is modulated at 100 kHz with $\beta = 0.34$ (see Fig. 4(a)). A 4-fold division by an EFD results in discrete sidebands of the same spacing but reduced amplitudes, as shown in Fig. 3(b). This result is consistent with theoretical calculations based on (10). Fig. 4(c)–(f) represent the case of WBFM, with a modulation frequency of 1 kHz and an FM frequency deviation of 242 kHz (that is $\beta = 242$). The original spectrum (see Fig. 4(c)) is a quasi-continuous, flattop sideband extending up to about 250 kHz. As the signal goes through the EFDs, the spectral width is reduced according to the division ratio but the overall profile of the sideband remains approximately the same, as demonstrated in Fig. 4(d) and (e). However, when the divided β becomes comparable to 1 (in this case when $N = 128$), the divided spectrum begins to transform into a series of discrete sidebands at the harmonics of 1 kHz, as shown in Fig. 4(f), which resembles a NBFM spectrum. Once again, these experimental results agree well with theoretical predictions. We have also investigated multi-tone modulations with independently controlled parameters and the results are generally simple combinations of the above two special cases. Finally, Fig. 4(g) and (h) show the case of BBPM, where the modulation consists of a continuous band of frequencies, all at low modulation indices. The measured result indicates that a 4-fold division causes the entire sideband to lower by 12 dB (see Fig. 4(h)). This is in good agreement with the theoretical prediction based on (13).

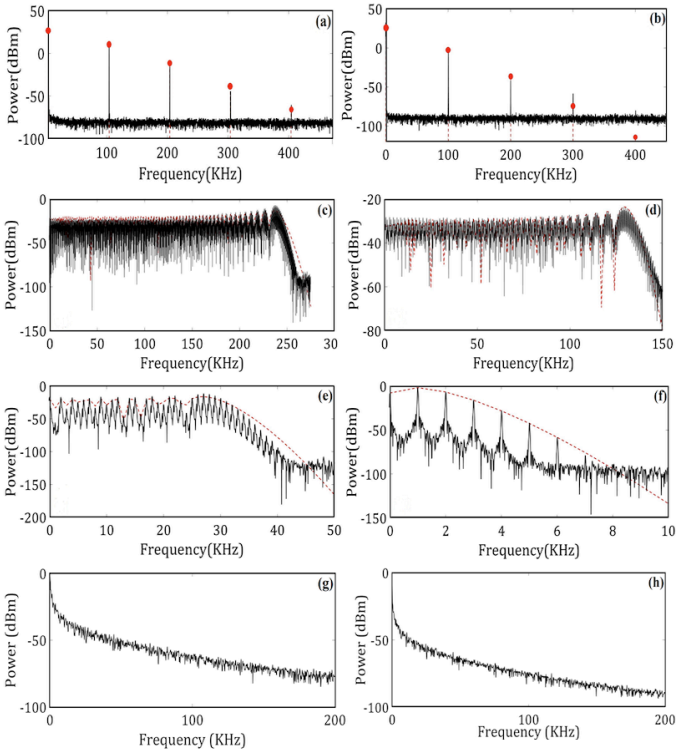

Fig. 4. The responses of EFD to various types of angle modulation: experimental (solid black) vs. theoretical (dashed red). (a) and (b): NBFM (undivided and divided by 4, respectively). (c)–(f): WBFM (undivided, divided by 2, 8, and 128, respectively). (g) and (h): BBPM (undivided and divided by 4, respectively).

IV. Application

In order to put our scheme to the test under more realistic conditions, we deliberately generate a noisy RF spectrum by beating a diode laser (DL) with an optical frequency comb (OFC). Such a beat note is frequently used in practice to facilitate DL-OFC locking [13]. Understanding the physical mechanisms behind the PFN of the beat note is essential to designing proper locking systems. In the current case, the diode laser is the same narrow linewidth laser mentioned above. The OFC (Menlo Systems FC1500) has a 250-MHz repetition rate, which is stabilized against a Rubidium frequency standard (SRS FS725). The carrier-envelope offset (CEO) frequency, however, is not stabilized. The RF beat note feeds into the two EFDs under various division-ratio settings, producing a series of spectra, which are summarized in Fig. 5. Fig. 5(a) shows the PSD spectra of the original beat note as well as the beat note divided by 4, 8, 16 and 32. All traces are re-centered to frequency zero for the sake of comparison. The undivided beat note features a flattop profile across over 300 kHz. As the division ratio gradually increases, the bandwidth of the beat note decreases in proportion, displaying a WBFM behavior similar to those shown in Fig. 2(b) and Fig. 3(c)–(e). It should be noted that the small sidebands in Fig. 5(a) at about 44 kHz and 87 kHz are introduced by the dividers as opposed

to the beat note. Increasing the division ratio further, the trend of linewidth reduction continues, as shown in Fig. 5(b) for N = 64, 128 and 256. A close look at the center regions of all these traces reveals a similar flattop feature, suggesting that the divided β remains large throughout the frequency division thus far and the divided beat note maintains its WBFM nature. However, when the division ratio is raised to 512, a set of discrete peaks at the harmonics of 1.8 kHz appears (upper trace in Fig. 5(c)). In addition, possible NBFM sidebands emerge at about 180 Hz from the carrier peak (upper trace in Fig. 5(c) inset). Finally, at N = 1024, the peaks at the harmonics of 1.8 kHz remain at the same frequencies but their amplitudes reduce by about 6 dB (lower trace in Fig. 5(c)), confirming their NBFM nature. Meanwhile, several other NBFM sidebands are clearly revealed at lower frequencies, including ones near 180 Hz, 300 Hz, 420 Hz, 620 Hz and 920 Hz (lower trace in Fig. 5(c) inset).

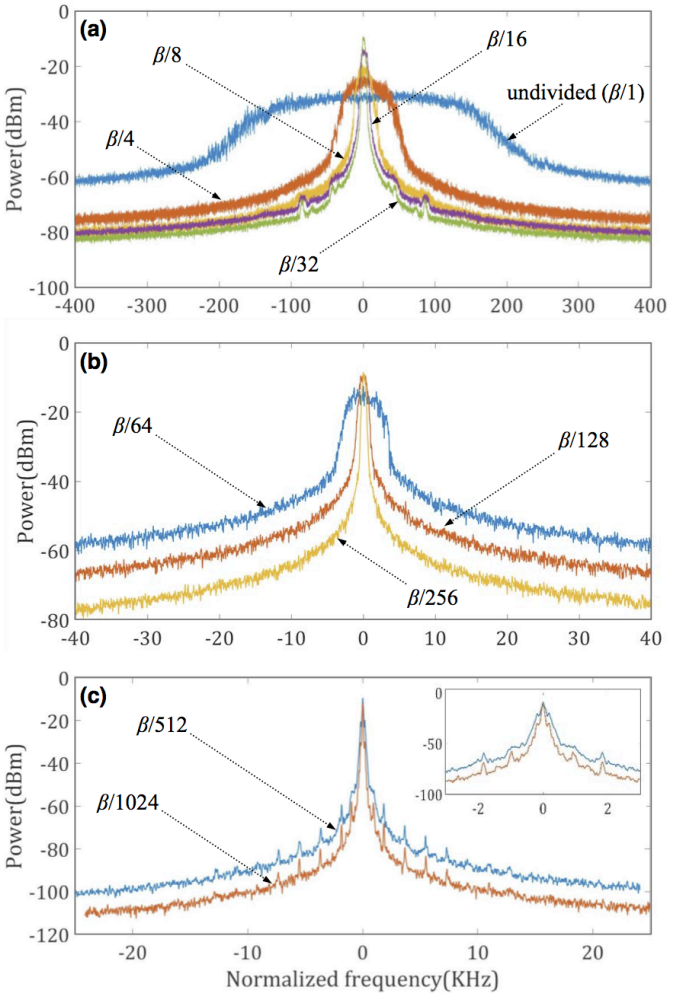

Fig. 5. Frequency-divided beat note between the DL and the OFC for division ratios of (a) 1 (undivided), 4, 8, 16 and 32; (b) 64, 128 and 256; (c) 512 and 1024. Instrument resolution bandwidths are (a) 50 Hz, (b) 50 Hz and (c) 40 Hz.

Further increasing the division ratio is currently not feasible due to the availability of EFDs. However, the analysis so far has yielded valuable insights into the properties of the beat note. The original beat note is predominantly WBFM-broadened, and there are multiple FM mechanisms tracing back to the lasers. The most prominent FM frequencies are at about 180 Hz and 1.8 kHz. As to the other sideband frequencies, e.g., 300 Hz, 420 Hz, 620 Hz and 920 Hz, the current spectral resolution and measurement precision are inadequate to determine whether they belong to the same series as the 180-Hz modulation or other independent modulations. However, it is evident that the sideband near 180 Hz is by far the strongest among all resolvable sidebands. It is therefore reasonable to assume the roughly 300-kHz initial linewidth of the beat note is primarily caused by this low-frequency modulation, which implies a modulation depth Δf of about 150 kHz and modulation index β of approximately 830. This result is consistent with the fact that the 180-Hz sideband appears only when N reaches above 512. Since the EFDs divide the modulation indices for different modulation frequencies with exactly the same ratio, we can also estimate the β associated with the 1.8-kHz FM based on the difference between the 180-Hz peak and the 1.8-kHz peak, which is about 40 dB according to Fig. 5(c) inset. This leads to an estimation of $\beta = 8$ for the FM at 1.8 kHz. All these above findings appear to agree with our understanding of the physical sources of fluctuations in the current circumstance. The broadening of the beat note is primarily due to the broadening of the OFC comb lines near the OFC center wavelength 1550 nm, which is mainly attributed to environmental noise (e.g., cavity length fluctuations) at frequencies below a few kilohertz [18]. Our method not only determines the FM frequencies but also their modulation indices as well.

It should be noted that both the DL and the CEO frequency of the OFC are free-running in this experiment. As a result, the beat note constantly drifts throughout the data-acquisition process. Such a drift would have greatly hindered the conventional techniques for high-resolution spectral analysis (e.g., fast Fourier transform (FFT) analysis). Yet our method demonstrates a high degree of robustness under frequency drift and displays a capability of capturing fine spectral details without the need of extensive frequency stabilization.

V. Conclusion

EFD-aided laser frequency analysis has been proposed and demonstrated here as an effective solution to improve the specificity of conventional spectral analysis based on direct PSD measurement. By applying frequency division prior to PSD measurement and monitoring the spectral changes caused by the EFD, one can differentiate common PFN situations such as WBFM and BBPM without ambiguity. Moreover, the new method allows for quantitative determination of WBFM parameters such as modulation frequency, modulation index and FM frequency deviation, which is not possible with any conventional spectral analysis methods. These additional capabilities can be of great benefit to the development of laser frequency locking systems. It can also find applications in a breadth of fields including RF photonics, optical sensing, radar/lidar, etc.

REFERENCES

[1] T. W. Hansch, "Nobel Lecture: Passion for precision," *Rev. Mod. Phys.*, vol. 78, no. 4, pp. 1297-1307, Dec. 2006.

[2] H. Ludvigsen, M. Tossavainen, and M. Kaivola, "Laser linewidth measurement using self-homodyne detection with short delay," *Opt. Commu.,* vol. 155, no. 1-3, pp. 180-186, June 1998.

[3] T. Okoshi, K. Kikuchi, and A. Nakayama, "Novel method for high resolution measurement of laser output spectrum," *Electronics Lett.,* vol. 16, no. 16, pp. 630-631, July 1980.

[4] E. Rubiola, E. Salik, S. Huang, N. Yu, and L. Maleki, "Photonic-delay technique for phase-noise measurement of microwave oscillators," *J. Opt. Soc. Am. B*, vol. 22, no. 5, pp. 987-997, May 2005.

[5] T. Duthel, G. Clarici, R. S. Fludger., J. C. Geyer, C. Schulien, and S. Wiese, "Laser linewidth estimation by means of coherent detection," *IEEE Photonics Tech. Lett.,* vol. 21, no. 20, pp. 1568-1570, Oct. 2009.

[6] J. F. Cliche, Y. Painchaud, C. Latrasse, M. J. Picard, I. Alexandre, and M. Tetu (2007, Sept.), Quebec, Qc, Canada. Ultra-Narrow Bragg Grating for Active Semiconductor Laser Linewidth Reduction through Electrical Feedback. Presented at BGPP2007 Annual meeting. [Online] Available: https://www.osapublishing.org/abstract.cfm?uri=BGPP-2007-BTuE2

[7] R. W. P. Drever, J. L.Hall, F. V. Kowalski, J. Hough, G. M. Ford, A. J. Munley and H. Ward, "Laser Phase and Frequency Stabilization Using an Optical Resonator," *Appl.Phys. B,* vol. 31, no. 2, pp. 97-105, Feb 1983.

[8] A.P. Willis, A. I. Ferguson, and D. M. Kane, "Longitudinal mode noise conversion by atomic vapour," *Optics Commu.,* vol. 122, no. 1-3, pp. 31-34, Aug 1995.

[9] L.D. Turner, K. P. Weber, C. J. Hawthrone, and R. E. Scholten, "Frequency noise characterisation of narrow linewidth diode lasers," *Optics Commu.,* vol. 201, no. 4-6, pp. 391-397, Nov 2001.

[10] M. Schiemangk, S. Spieberger, A. Wicht, G. Erbert, G. Trankle and A. Peters "Accurate frequency noise measurement of free-running lasers," *Appl. Opt.,* vol. 53, no. 30, pp. 7138-7143, Oct. 2014.

[11] H.-H. Wu, G.-R. Lin and C.-L. Pan, "Optoelectronic phase tracking and electrooptic sampling of free-running microwave signals up to 20 GHz in a laser-diode-based system," *IEEE Photon. Tech. Lett.*, vol. 7, no. 6, pp. 670-672, Jun. 1995.

[12] G.-R. Lin, T.-S. Hwang, Y.-H. Chuang, S. C. Wang, and C-L. Pan, "Broad-band (⩾20 GHz) laser-diode-based optoelectronic microwave phase shifter," *IEEE Trans. Microwave Theory Tech.*, vol. 46, no. 10, pp. 1419-1426, Oct. 1998.

[13] J. Ye, H. Schnatz, and L. W. Hollberg, "Optical frequency combs: from frequency metrology to optical phase control," *IEEE J. Sel. topics in quantum elect.,* vol. 9, no. 4, pp. 1041-1058, Aug. 2003.

[14] L. Duan and K. Gibble, "Locking lasers with large FM noise to high-Q cavities," *Opt. Lett*., vol. 30, no. 24, pp. 3317-3319, Dec. 2005.

[15] W. F. Egan, "Modeling phase noise in frequency dividers," *IEEE Trans. Ultrason. Ferroelectrics and Frequency Control,* vol. 37, no. 4, pp. 307-315, July 1990.

[16] S. Levantino, L. Romano, S. Pellerano, C. Samori, and A. L. Lacaita "Phase noise in digital frequency dividers," *IEEE Journal of Solid-State Circuits*, vol. 39, no. 5, pp. 775-784, May 2004.

[17] B. Carlson, P. B. Crilly, J. C. Rutledge, "Exponential CW Modulation," in *Communication systems: An Introduction to Signals and Noise in Electrical Communication*, 4th ed., New York, NY, USA: McGraw-Hill, 2002, ch. 5, pp. 183-224.

[18] N. R. Newbury and W. C. Swann, "Low-noise fiber-laser frequency combs," *J. Opt. Soc. Am. B*, vol. 24, no. 8, 1756-1769, Aug. 2007.

Dipen Barot was born in Anand district of Gujarat state in India. He received the B.E. degree in Electronics and Communication Engineering from G. H. Patel College of Engineering and Technology, India, in 2009 and the M. Tech degree in Information and Communication Technology from Dhirubhai Ambani Institute of Information and Communication Technology, India, in 2013. He is currently pursuing a Ph.D. degree in Optical Science and Engineering at the University of Alabama in Huntsville, AL, USA.

From 2013 to 2014, he worked as an Assistant Professor in the Electronics and Communication Engineering Department at Dharmsigh Desai University, Gujarat, India. His current research interests include ultra-stable narrow linewidth optical sources, phase noise characterization methods of optical oscillators and fiber optics.

Lingze Duan (M'01–SM'14) was born in Beijing, China. He received the B.S. degree in physics from Tsinghua University, Beijing, China in 1995 and the Ph.D degree in electrical engineering from the University of Maryland, College Park, MD, USA in 2002.

From 2002 to 2004, he was a Post-Doctoral Associate with the Research Laboratory of Electronics (RLE), Massachusetts Institute of Technology, Cambridge, MA, where he conducted research on octave-spanning optical pulse generation and characterization. From 2004 to 2007, he was a post-doctoral researcher with the Department of Physics, Pennsylvania State University, University Park, where he developed ultrastable diode laser systems based on high-Q optical cavities. He joined the Department of Physics, University of Alabama in Huntsville, Huntsville, AL, as a faculty member, in 2007, where he has been an Associate Professor since 2013. He has published over 50 refereed technical publications. His research interest includes ultrafast nanophotonics, frequency metrology with femtosecond frequency combs, fiber optic sensors, and novel applications of optics in astrophysics.

Dr. Duan was a recipient of the National Science Foundation Faculty Early Career Development (CAREER) Award in 2013. He is a Senior Member of IEEE and a Senior Member of the Optical Society (OSA).